Int. J. Multiphase Flow Vol. 18, No. 6, pp. 787–801, 1992
Printed in Great Britain.

0301-9322/92 $5.00 + 0.00

THE USE OF DRIFT-FLUX TECHNIQUES FOR THE ANALYSIS OF HORIZONTAL TWO-PHASE FLOWS

F. FRANÇA† and R. T. LAHEY JR
Center for Multiphase Research, Rensselaer Polytechnic Institute, Troy, NY 12180-3590, U.S.A.

(Received 6 August 1990; in revised form 5 September 1992)

Abstract—New data is presented for horizontal air/water two-phase flow having various flow regimes. It is shown that drift-flux models are able to correlate these data and that the drift velocity, V_{Gj}, is normally finite.

Key Words: flow regime, drift-flux, horizontal two-phase flow

INTRODUCTION

The drift-flux model has been widely used for the calculation of void fraction and other constitutive relations in vertical gas/liquid two-phase flows. However, the model proposed by Zuber & Findlay (1965) is a general model which does not depend explicitly on conduit orientation. Nevertheless, the drift-flux parameters C_0 and V_{Gj}, should depend on the flow orientation and flow regime in gas/liquid flows.

For vertical flows, the drift velocity, V_{Gj}, results from a balance between the local interfacial drag and the buoyancy on the dispersed phase. This is not the case for horizontal flows. The drift velocity in these flows is related to the phase distribution and to the local slip resulting from the lateral and axial pressure gradients. Moreover, in separated horizontal flows the structure of the interface determines the drift-flux parameters.

A review of the literature shows that two different methods have been used to correlate the void fraction (or equivalently, the liquid holdup) in a horizontal two-phase flow. A completely empirical approach was used in the works of Armand (1946), Lockhart & Martinelli (1949), Beggs (1972), Gouvier & Omer (1962) and Spedding & Chen (1984), among many others. In those works the independent variables chosen to show the relationship between the void fraction and flow parameters can, as discussed by Butterworth (1975), be deduced from a simple homogeneous model. A particular set of variables which have been successfully used are the gas/liquid volume fraction ratio, $\langle \varepsilon \rangle/(1-\langle \varepsilon \rangle)$, and the gas/liquid superficial velocity ratio, $\langle j_G \rangle/\langle j_L \rangle$. These parameters are a particularly good choice for correlating data in which there is a large difference between the superficial velocities (i.e. for the wavy/stratified and annular flow regimes).

Phenomenological models have also been developed to calculate the void fraction in horizontal flows. When applied to particular flow patterns, these models attempt to overcome the limitations related to completely empirical models and extend the results to a broad range of pipe sizes, fluid properties and flow conditions. The models of Taitel & Dukler (1976), Nguyen & Spedding (1977), Cheremisinoff & Davis (1979), Chen & Spedding (1983), Andreussi & Persen (1987) and Hart *et al.* (1989) are typical of the phenomenological approach. Despite the mechanistic basis of the phenomenological approaches, all of these models still depend on empirical parameters, and show good agreement with experiments only for limited flow conditions.

ANALYSIS

Another phenomenological approach, which has been widely used for vertical two-phase flows, but not for horizontal two-phase flows, is the drift-flux model (Zuber & Findlay 1965). It is the

†Currently at: Universidade Estadual de Campinas—UNICAMP, São Paolo, Brazil.

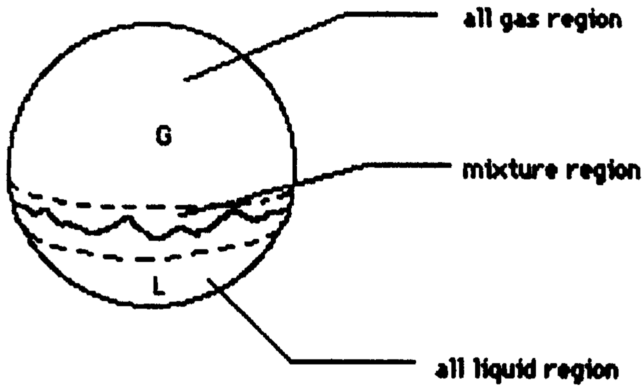

Figure 1. Flow pattern in wavy–stratified horizontal gas/liquid flow (cross-sectional view).

purpose of this paper to discuss how data from horizontal gas/liquid flows can be correlated using a drift-flux model. To this end, new horizontal two-phase flow data were taken. To validate these experiments and better define the trends observed, these new data were compared to other data and the results from many of the correlations and models mentioned above.

The Zuber–Findlay (1965) drift-flux model implies a linear relationship, between the average gas velocity, $\langle v_G \rangle_G$, and the average volumetric flux $\langle j \rangle$:

$$\langle v_G \rangle_G = \frac{\langle j_G \rangle}{\langle \varepsilon \rangle} = C_0 \langle j \rangle + V_{Gj}. \quad [1]$$

In [1], $\langle v_G \rangle_G$ is the averaged gas velocity (Lahey & Moody 1977), $\langle j_G \rangle$ is the superficial gas velocity and $\langle \varepsilon \rangle$ is the global void fraction. The volumetric flux, $\langle j \rangle$, is the sum of the gas and liquid superficial velocities (i.e. $\langle j \rangle = \langle j_G \rangle + \langle j_L \rangle$). The so-called distribution parameter, C_0, and the drift velocity, V_{Gj}, are defined as

$$C_0 = \frac{\langle \varepsilon j \rangle}{\langle \varepsilon \rangle \langle j \rangle} \quad [2]$$

and

$$V_{Gj} = \frac{\langle \varepsilon (v_G - j) \rangle}{\langle \varepsilon \rangle} = \frac{\langle \varepsilon (1 - \varepsilon) v_r \rangle}{\langle \varepsilon \rangle}. \quad [3]$$

The symbol $\langle \ \rangle$ represents averaging over the pipe cross-sectional area and v_r is the local relative velocity, $(v_G - v_L)$. Correlating data using [1] is appropriate for quasi-steady flows having superficial velocities which are similar in magnitude (e.g. for intermittent flows). In contrast, for separated air/water horizontal flows, the ratio $\langle j_G \rangle / \langle j_L \rangle$ can be so high that the usual graphical method for determining C_0 and V_{Gj} does not show sufficient sensitivity to changes in $\langle j_L \rangle$.

For such cases, [1] can be rewritten as

$$\frac{1 - C_0 \langle \varepsilon \rangle}{\langle \varepsilon \rangle} = \frac{1}{\langle j_G \rangle} (C_0 \langle j_L \rangle + V_{Gj}) \quad [4]$$

or, if the drift velocity, V_{Gj}, is given by (Lahey & Moody 1977)

$$V_{Gj} = V'_{Gj} - (C_0 - 1) \langle j \rangle, \quad [5]$$

[4] may be rewritten as

$$\frac{1 - C_0 \langle \varepsilon \rangle}{\langle \varepsilon \rangle} = \frac{1}{\langle j_G \rangle} (C_0 \langle j_L \rangle + V'_{Gj} - (C_0 - 1) \langle j \rangle). \quad [6]$$

The generalized drift velocity, V'_{Gj}, is related to the phase-averaged relative velocity by

$$V'_{Gj} = (1 - \langle \varepsilon \rangle)(\langle v_G \rangle_G - \langle v_L \rangle_L). \quad [7]$$

Table 1

Gauge pressure (mH_2O)	$\langle j_G \rangle$ (m/s)	$\langle j_L \rangle$ (m/s)	$\langle j \rangle$ (m/s)	$\langle \varepsilon \rangle$ (%)	$\langle v_G \rangle_G$ (m/s)	C_0	Flow regime (stratified)
0.00	3.06	0.0056	3.07	93	3.29	1.07	Smooth
0.00	3.12	0.0166	3.14	89	3.53	1.12	Smooth/wavy
0.20	9.61	0.042	9.65	89	10.84	1.12	Wavy
0.26	15.57	0.042	15.61	92	16.89	1.08	Wavy

To evaluate [6], one must specify the distribution parameter, C_0, and the generalized drift velocity, V'_{Gj}. The specification of C_0 requires that one know the phase distribution. Unfortunately, this is not generally known. Nevertheless, based on an analysis of idealized horizontal flows it is possible to estimate limiting values for C_0 and to infer the trend as the flow variables change. To accomplish this, let us follow an approach similar to that adopted by Nguyen & Spedding (1977), and consider three different regions for the wavy-stratified flow shown in figure 1. From the definition of C_0, we can write

$$C_0 = \frac{1}{A_{x\text{-}s}\langle \varepsilon \rangle \langle j \rangle}\left(\int_{A_G} \varepsilon j \, dA + \int_{A_m} \varepsilon j \, dA + \int_{A_L} \varepsilon j \, dA\right), \qquad [8]$$

where the subscripts G, L and m denote the all gas, all liquid and mixture regions, respectively, and $A_{x\text{-}s}$ is the pipe's cross-sectional area.

If there is no vapor carry-under, the integral over the all liquid region vanishes (since $\varepsilon = 0$ there), and if one assumes a very thin mixture region compared to the pipe section (i.e. $A_m/A_{x\text{-}s} \ll 1$), which is characteristic of stratified flow, C_0 is well-approximated by

$$C_0 \cong \langle v_G \rangle_G / \langle j \rangle. \qquad [9]$$

To calculate C_0 from [9] for a given gas and liquid flow rate, the void fraction has to be calculated, since $\langle v_G \rangle_G = \langle j_G \rangle / \langle \varepsilon \rangle$. The void fraction in a stratified flow is related to the forces acting on the liquid and gas phases. For steady, fully developed horizontal two-phase flows, the interfacial drag is balanced by the axial pressure gradient and shear stresses at the wall. The equations expressing this balance can be simultaneously solved if reasonable assumptions are made (Taitel & Dukler 1976). If the liquid film has a smooth surface, the gas can be considered to flow in a smooth pipe and the stratified liquid level or, equivalently, the global void fraction, can be given as a function of χ^2,

$$\langle \varepsilon \rangle = \langle \varepsilon(\chi^2) \rangle, \qquad [10]$$

where χ^2 is the well-known Martinelli parameter, which is the ratio of the liquid/gas pressure gradients based on their respective superficial velocities. The specific functional form in [10] depends on their respective superficial velocities and whether the single-phase gas and liquid regimes are laminar or turbulent. Andreussi & Persen (1987) compared [10] to their measurements. For stratified-smooth flows they found good agreement. Values for C_0, calculated from [9] and [10], are shown in table 1 for some stratified flow data taken in our experiments. As can be seen, reasonable values of C_0 are predicted.

It is worthwhile mentioning that the Taitel–Dukler (1976) model is known to underpredict the global void fraction in the wavy region. As a consequence, the values for C_0 given in table 1 for that flow regime may be somewhat lower than actual. Nevertheless, considering that the values obtained for C_0 are near unity, [6] can be approximated as

$$\frac{\langle \varepsilon \rangle}{1 - \langle \varepsilon \rangle} \cong \frac{1}{(1+K)} \frac{\langle j_G \rangle}{\langle j_L \rangle}, \qquad [11]$$

where

$$K = \langle V'_{Gj} \rangle / \langle j_L \rangle. \qquad [12]$$

Equation [11] can be conveniently used to correlate data for horizontal stratified-smooth, wavy and annular flow regimes. Obviously, the closer C_0 is to unity, the better the results.

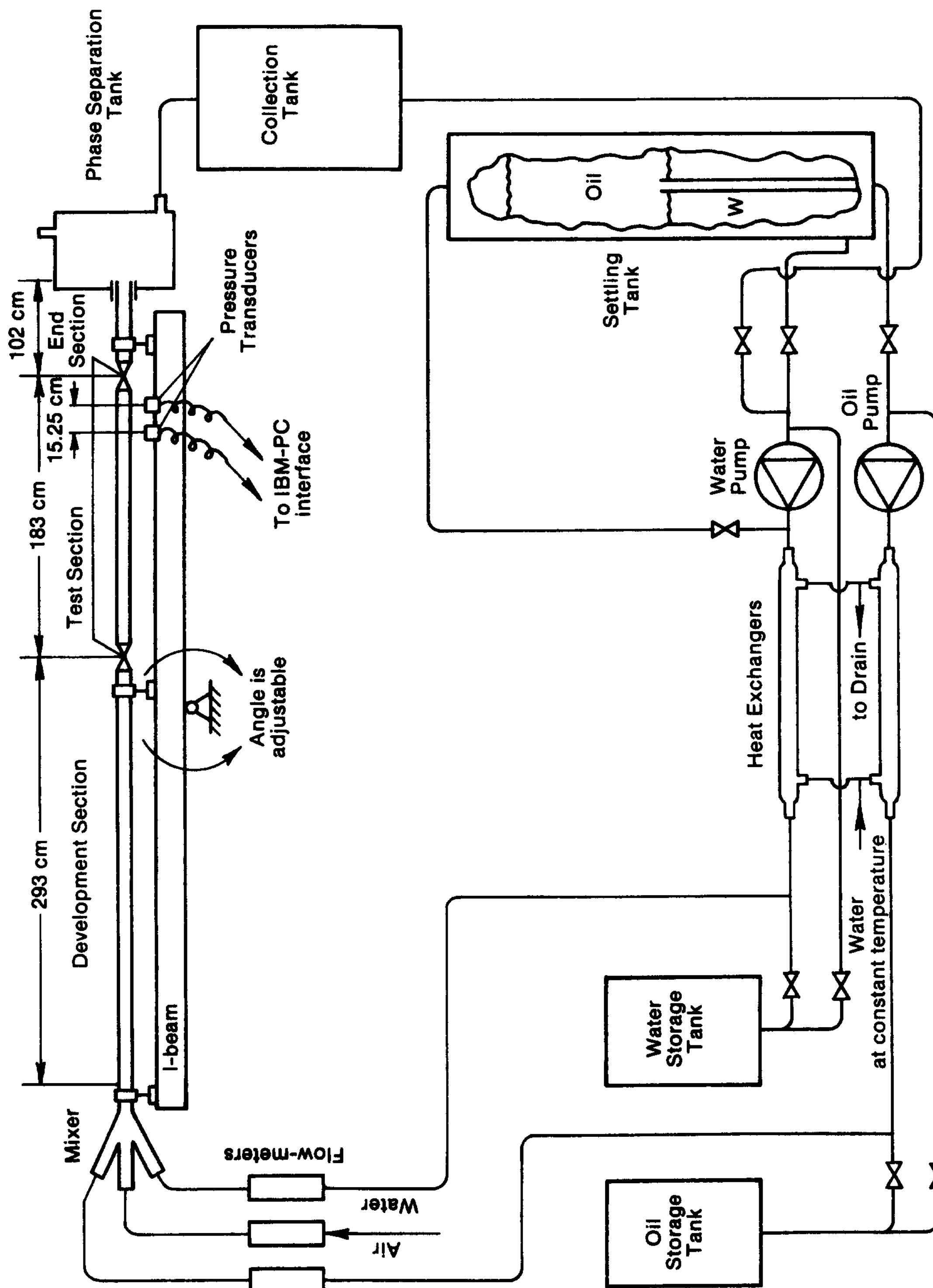

Figure 2. Schematic of the RPI test loop.

Table 2

Run No.	Gauge pressure (mH_2O)	$\langle j_G \rangle$ (m/s)	$\langle j_L \rangle$ (m/s)	$\langle \varepsilon \rangle$ (%)	Flow regime
1	0.00	1.564	0.0056	65.0	Stratified-smooth/wavy
2	0.00	2.086	0.0056	73.4	Stratified-smooth/wavy
3	0.00	2.607	0.0056	81.8	Stratified-smooth/wavy
4	0.00	3.129	0.0056	88.1	Stratified-smooth/wavy
5	0.00	3.650	0.0056	89.5	Stratified-smooth/wavy
6	0.00	2.086	0.0166	65.7	Stratified-smooth/wavy
7	0.00	2.607	0.0166	71.3	Stratified-smooth/wavy
8	0.00	3.129	0.0166	81.8	Stratified-smooth/wavy
9	0.00	3.650	0.0166	83.2	Stratified-smooth/wavy
10	0.00	4.172	0.0166	84.6	Stratified-smooth/wavy
11	0.00	5.215	0.0166	87.4	Stratified-smooth/wavy
12	0.00	2.067	0.0299	67.1	Stratified-smooth/wavy
13	0.00	3.129	0.0299	72.0	Stratified-smooth/wavy
14	0.00	3.650	0.0299	74.8	Stratified-smooth/wavy
15	0.02	9.616	0.0428	90.9	Stratified-smooth/wavy
16	0.06	12.653	0.0428	92.3	Stratified-smooth/wavy
17	0.14	15.577	0.0428	94.4	Stratified-smooth/wavy
18	0.13	11.722	0.1257	88.1	Stratifying-annular
19	0.18	13.665	0.1257	88.8	Stratifying-annular
20	0.30	17.187	0.1257	91.3	Stratifying-annular
21	0.49	21.115	0.1257	93.0	Stratifying-annular
22	0.26	6.494	0.2771	79.0	Stratifying-annular
23	0.30	9.851	0.2771	80.4	Stratifying-annular
24	0.43	13.574	0.2771	83.2	Stratifying-annular
25	0.62	16.905	0.2771	86.7	Stratifying-annular
26	1.05	20.124	0.2771	88.8	Stratifying-annular
27	1.47	23.760	0.2771	91.3	Stratifying-annular
28	0.20	0.253	0.6596	25.9	Plug
29	0.22	0.505	0.6596	38.5	Plug
30	0.25	0.755	0.6596	47.6	Plug
31	0.27	1.003	0.6596	58.7	Slug
32	0.27	1.254	0.6596	54.5	Slug
33	0.27	1.254	0.6596	54.5	Slug
34	0.25	1.007	0.6596	58.7	Slug
35	0.22	0.757	0.6596	57.3	Slug
36	0.22	0.757	0.6596	49.7	Slug
37	0.21	0.505	0.6596	42.0	Slug
38	0.20	0.253	0.6596	27.3	Slug
39	0.25	0.251	0.8256	20.3	Plug
40	0.27	0.501	0.8256	32.9	Plug
41	0.29	0.750	0.8256	47.9	Slug
42	0.33	0.996	0.8256	51.7	Slug
43	0.35	1.282	0.8256	52.1	Slug
44	0.38	1.580	0.8256	55.2	Slug
45	0.40	1.840	0.8256	58.7	Slug
46	0.40	1.840	0.8256	58.7	Slug
47	0.38	1.580	0.8256	55.2	Slug
48	0.35	1.282	0.8256	53.1	Slug
49	0.33	0.996	0.8256	52.4	Slug
50	0.41	1.838	0.8256	58.7	Slug
51	0.41	1.838	0.8256	58.7	Slug
52	0.41	1.838	0.8256	58.7	Slug
53	0.41	1.838	0.8256	58.7	Slug
54	0.43	2.094	0.8256	62.2	Slug
55	0.43	2.094	0.8256	62.2	Slug
56	0.43	2.094	0.8256	62.2	Slug
57	0.45	2.348	0.8256	65.0	Slug
58	0.45	2.348	0.8256	65.0	Slug
59	0.45	2.348	0.8256	65.0	Slug
60	0.13	1.023	0.0056	60.8	Stratified-smooth/wavy
61	0.14	4.085	0.0428	79.7	Stratified-smooth/wavy
62	0.14	4.851	0.0428	80.8	Stratified-smooth/wavy
63	0.16	6.119	0.0428	86.0	Stratified-smooth/wavy
64	0.16	6.629	0.0428	88.1	Stratified-smooth/wavy
65	0.17	8.145	0.0428	90.2	Stratified-smooth/wavy
66	0.19	10.489	0.0428	91.6	Stratified-smooth/wavy
67	0.14	0.127	0.1981	27.3	Plug

continued overleaf

Table 2—*continued*

Run No.	Gauge pressure (mH_2O)	$\langle j_G \rangle$ (m/s)	$\langle j_L \rangle$ (m/s)	$\langle \varepsilon \rangle$ (%)	Flow regime
68	0.14	0.127	0.1981	27.3	Plug
69	0.14	0.127	0.1981	27.3	Plug
70	0.14	0.127	0.1981	27.3	Plug
71	0.16	0.127	0.3628	17.8	Plug
72	0.16	0.127	0.3628	18.2	Plug
73	0.18	0.127	0.6596	14.0	Plug
74	0.18	0.127	0.6596	15.4	Plug
75	0.30	0.249	1.1028	15.7	Plug
76	0.34	0.497	1.1028	29.7	Plug
77	0.38	0.766	1.1028	36.0	Slug
78	0.42	1.048	1.1028	48.3	Slug
79	0.45	1.324	1.1028	50.0	Slug
80	0.54	1.327	1.4853	42.3	Slug
81	0.52	1.049	1.4853	37.1	Slug
82	0.50	0.778	1.4853	31.5	Plug
83	0.45	0.521	1.4853	26.2	Plug
84	0.38	0.259	1.4853	13.6	Plug
85	0.35	0.128	1.4853	6.3	Plug
86	0.62	1.890	1.4853	50.3	Slug
87	0.62	1.890	1.4853	51.4	Slug
88	0.28	15.335	0.1257	89.5	Stratifying-annular
89	0.45	18.992	0.1257	91.6	Stratifying-annular
90	0.38	11.660	0.2771	81.1	Stratifying-annular
91	0.59	15.115	0.2771	85.0	Stratifying-annular
92	0.86	18.456	0.2771	88.1	Stratifying-annular
93	1.14	22.267	0.2771	90.2	Stratifying-annular
94	0.00	4.693	0.0056	93.0	Stratified-smooth/wavy
95	0.00	5.736	0.0056	93.7	Stratified-smooth/wavy
96	0.00	4.432	0.0056	93.0	Stratified-smooth/wavy
97	0.00	4.172	0.0299	81.8	Stratified-smooth/wavy
98	0.00	5.215	0.0299	82.5	Stratified-smooth/wavy
99	0.00	6.258	0.0299	86.7	Stratified-smooth/wavy

It is important to note that particular forms of [11] have been used previously to correlate data, with no physical justification. Also, the same form was analytically derived by Hart *et al.* (1989) for stratified and annular flows, applying a momentum balance to the two phases. In their case the equation parameter K was found to be

$$K = (\langle \varepsilon \rangle f_L \rho_L / f_i \rho_G)^{1/2}$$

and f_L/f_i, the ratio of the wall friction factor of the liquid phase to the interfacial friction factor, was calculated as a function of $\langle j_L \rangle$. This result is particularly suitable when the liquid and interfacial shear stress are the dominant process in the momentum exchange, as they are for wavy and annular flows.

Equations [7] and [12] imply a physical meaning for the parameter K, showing that it is related to the relative velocity. Thus, we expect it to be a function of flow regime and fluid properties.

DISCUSSION OF THE EXPERIMENT

A schematic of the three-phase (air/oil/water) test loop used in this study is shown in figure 2. It should be noted that in this study only air and water were used. Most of the development section and the test section comprised a 19 mm i.d. Plexiglas pipe. Some copper pipes of the same diameter were also used and special holders linked them to the supporting I-beam. The development section was 187 L/D long, so that a fully developed flow was achieved at the site of the pressure-drop measurement taps. The test section itself was 71.5 L/D long and the exit section, 55 L/D long. The mixture was discharged into a separation tank, which was at atmospheric pressure.

The water was routed to the inlet of the development section via an air/water mixer. As most of the water was recirculated in a high-pressure flow loop, the test section received a very stable water flow rate. Four parallel-connected calibrated Dwyer Ratemaster flow meters were used to measure water flow rate.

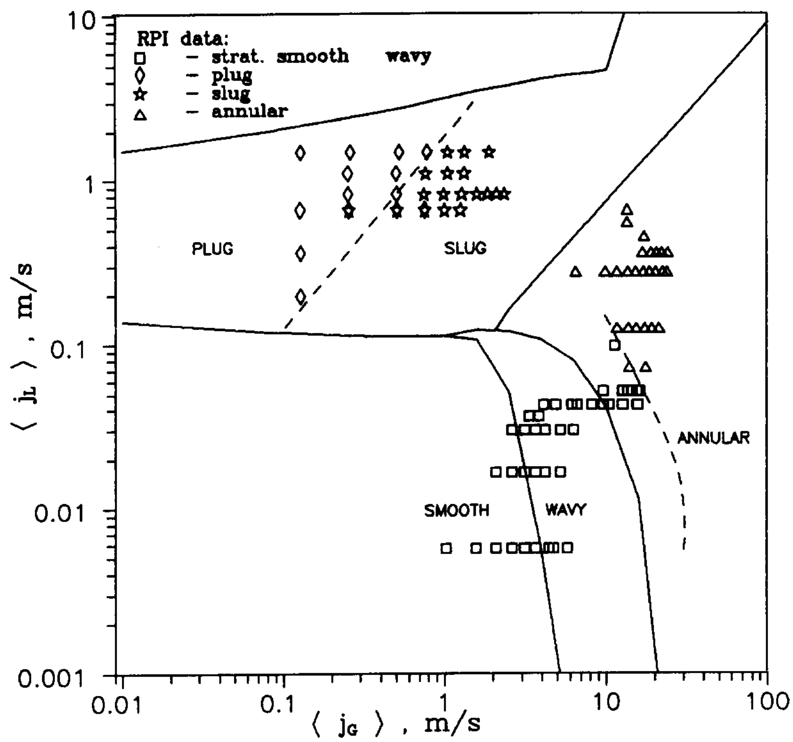

Figure 3. A comparison of the RPI data with the model of Taitel & Dukler (1976).

The air was routed into a mixer after passing through four parallel-connected calibrated Dwyer Ratemaster flow meters. Absolute pressure was measured at the inlet of the air flow meters, so that proper density corrections could be made. The loop was operated at room temperature, which was kept constant by using a heat exchanger connected to house water. The air inlet temperature was measured and used to correct the flow meter readings.

Pressure taps were mounted flush with the pipe for measuring the local pressure and pressure drop. A set of calibrated Validyne variable differential reluctance transducers, connected to Carrier demodulators, were used. A custom-built acquisition board was used for acquiring, digitizing and transferring the data to the memory of an IBM XT computer. The pressures were averaged over an appropriate time interval and used to compute the actual gas flow rate at the reference section (i.e. the middle of the test section).

The quick-closing valve method was used for the global void fraction measurements. The procedure adopted was to measure the global void fraction at least three times for each flow condition, in the wavy, plug, slug and annular regions. The results were then ensemble averaged. The accuracy of these results was estimated to be $\pm 5\%$ of point.

To distinguish between the flow patterns various methods were used. In particular, direct visual observation of the phase distribution for low flow rates, observation of the pressure and pressure-drop fluctuations on the screen of an oscilloscope and comparison of the averaged values of pressure and pressure drop. High speed photography was also used, as required.

DISCUSSION OF RESULTS

A set of 200 horizontal air/water data points were taken, for four flow patterns: plug, slug, wavy–stratified and annular. For 101 of these points, the void fraction was not measured, the main objective being the proper identification of flow patterns. The remaining 99 data points are tabulated in table 2.

Figure 3 shows some points from the set, plotted in a j_G–j_L flow regime map. The solid lines represent Taitel & Dukler's (1976) phenomenological flow regime transitions for a similar system operating under the same conditions, using the constant interface friction factor of 0.0142

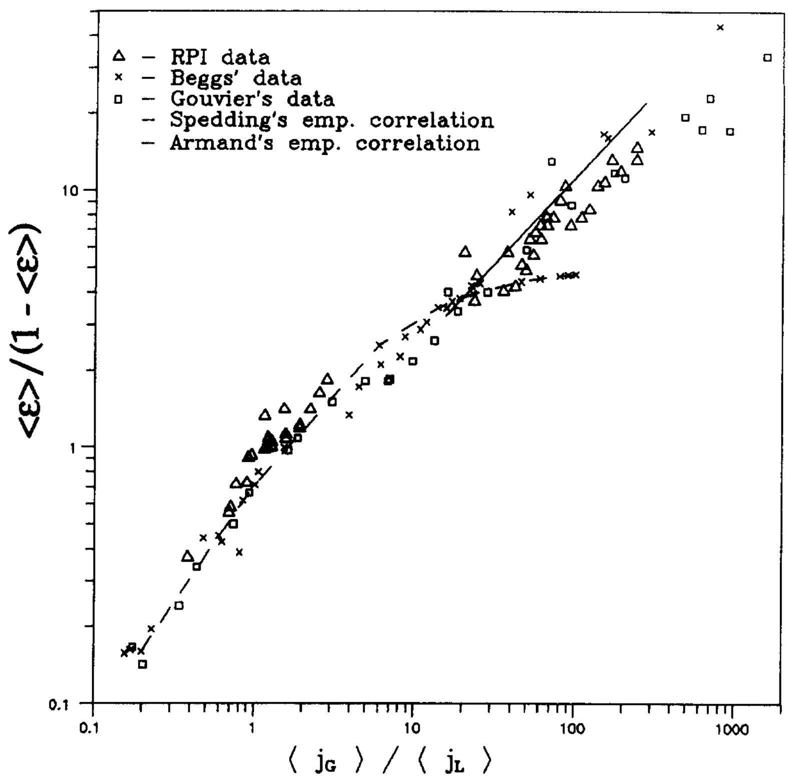

Figure 4. A comparison of the RPI data with other data and correlations.

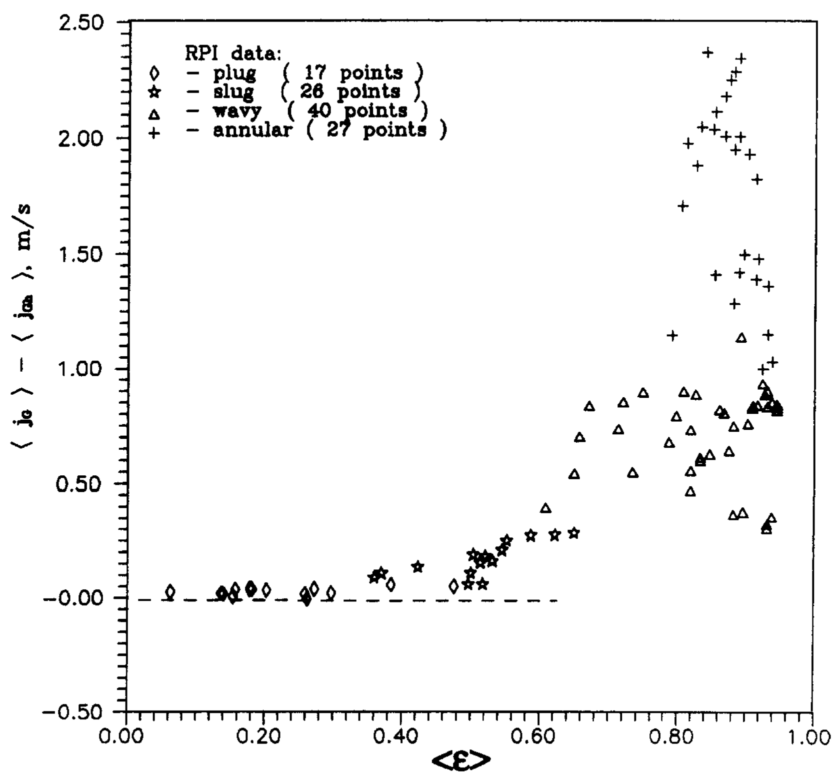

Figure 5. The classification of plug/slug flow.

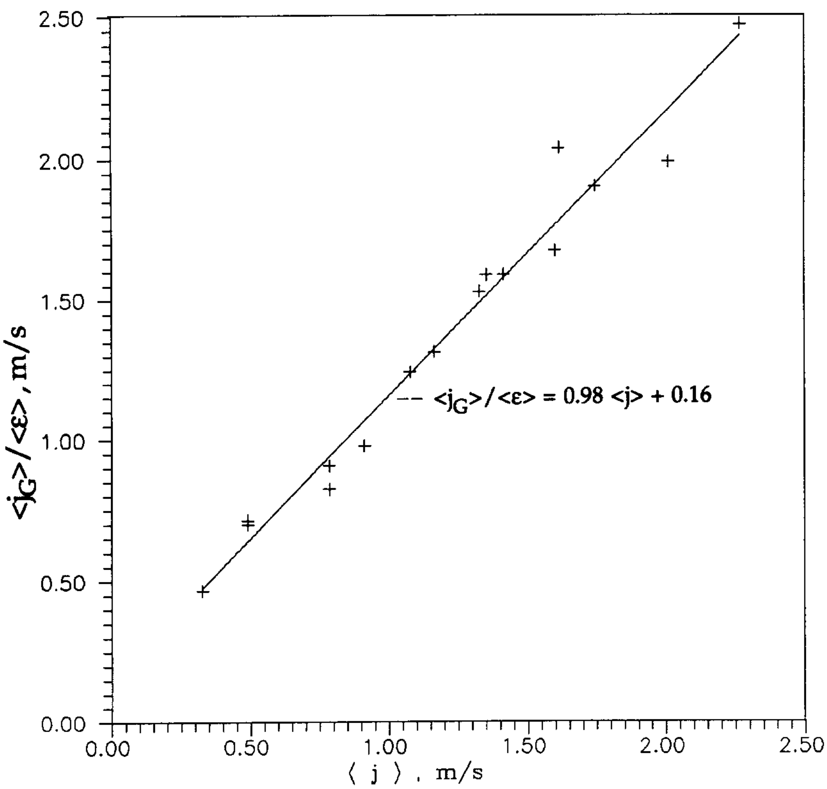

Figure 6. Plug flow data.

suggested by Shoham & Taitel (1984). The dashed lines represent the flow regime boundaries observed in this study. Despite some obvious differences between the data and the theoretical model, fairly good agreement was obtained.

To further demonstrate the correctness of the present data they are plotted in figure 4 with other data and correlations found in the literature; good agreement is seen. The other experiments were also for horizontal air/water flows, but the pipe diameter and flow conditions were not necessarily the same as in the present data.

Correlations for intermittent flows: plug and slug flow

To use a drift-flux model to correlate the intermittent horizontal patterns for plug and slug flow, one must first differentiate between them. The air bubble in the plug flow is bullet-shaped. Due to buoyancy, the bubble travels next to the upper wall of the conduit, and at low rates it shows a long tail, since it was driven by the liquid flow.

As the air flow rate increases, the regime becomes slug flow. The air bubbles between the liquid slugs becomes distorted and unstable. The interface of the liquid film on the bottom of the conduit is wavy, typical of an air-driven flow.

To distinguish between plug and slug flow an objective criterion, based on which phase drives the flow, was used. The actual gas superficial velocity, $\langle j_G \rangle$, was compared to the gas superficial velocity of a hypothetical "homogeneous" water-driven flow, given by $\langle j_G \rangle = \langle \varepsilon \rangle \langle j \rangle$. If $\langle j_G \rangle$ is approximately equal to $\langle j_{Gh} \rangle$, then the flow is said to be plug; otherwise it is classified as slug flow. In figure 5 the difference is said to be plug; otherwise, it is classified as slug flow. In figure 5 the difference between the superficial gas velocity and the "homogeneous" superficial gas velocity is plotted against the void fraction. Points with $(\langle j_G \rangle - \langle j_{Gh} \rangle) < 0.05$ m/s were classified as plug flow. This appears to occur in the range $\langle \varepsilon \rangle \leqslant 0.50$. It is interesting to note that [3] implies that in this range, $V_{Gj} \cong 0$.

In figure 6 data for plug flow is shown in terms of the drift-flux variables, $\langle j_G \rangle / \langle \varepsilon \rangle$ and $\langle j \rangle$. The solid line represents the best linear fit. The measured drift-flux parameters, C_0 and V_{Gj}, are 0.98 and 0.16 m/s, respectively. The distribution coefficient is slightly less than unity, indicating that

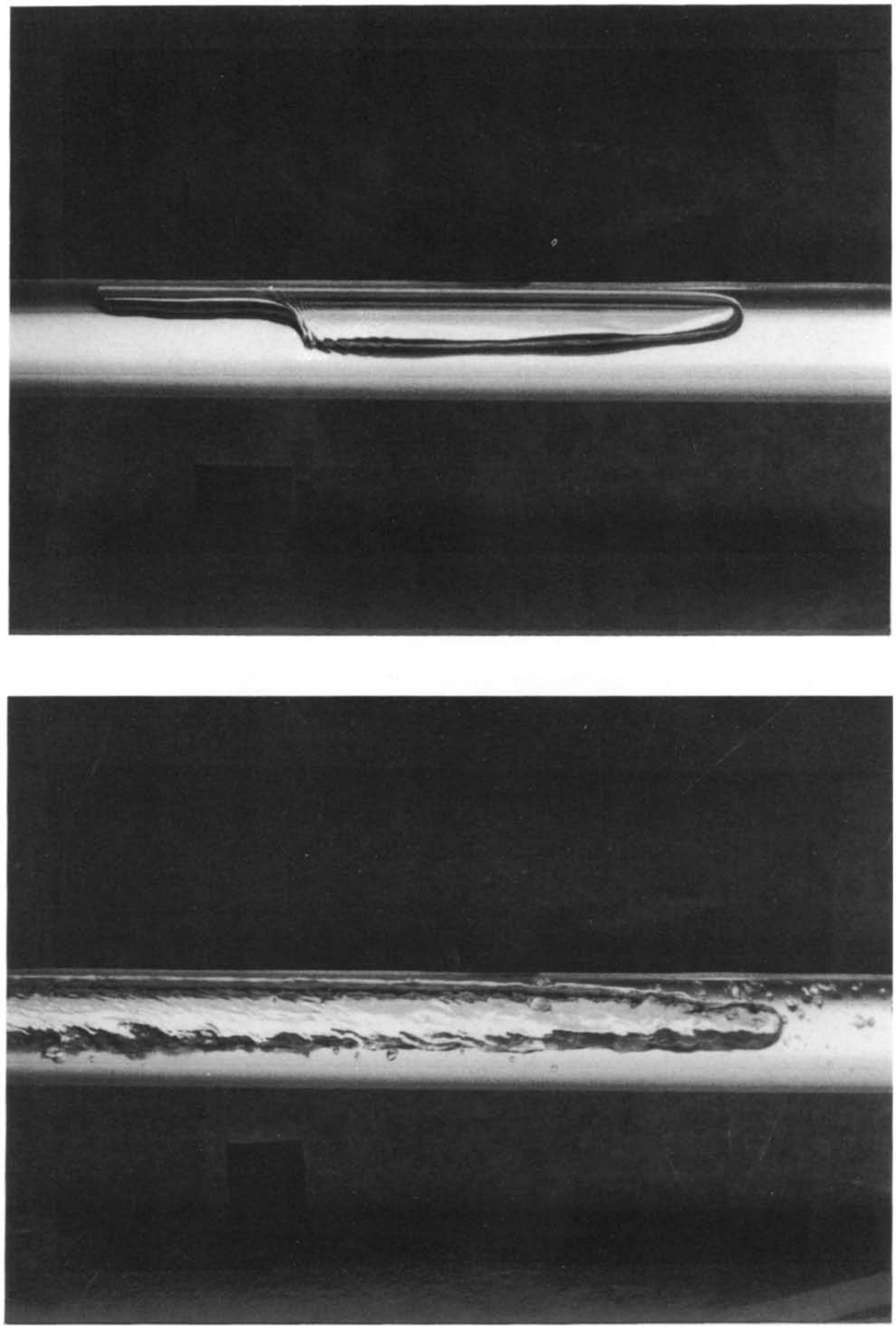

Figure 7. Plug and slug flow data: (a) plug flow (typical); (b) slug flow (typical).

the void profile is not completely in phase with the volumetric flux ($\langle j \rangle$) profile. In fact, the air bubbles are in contact with the upper conduit wall, thus most of them are in a region of lower liquid velocity. Interestingly, $V_{Gj} > 0$ for this horizontal flow regime.

It was observed that for plug flow the voids move as a unit, driven by the liquid, resulting in a small positive drift velocity. This is evident at low liquid flow rates, when surface tension still plays a role and the air bubbles shows a long, thin tail next to the upper pipe wall, figure 7(a). Our results for plug flow are supported by those obtained by Bendiksen (1984), who did experiments with long bubbles in air/water systems. These data show that the relationship between

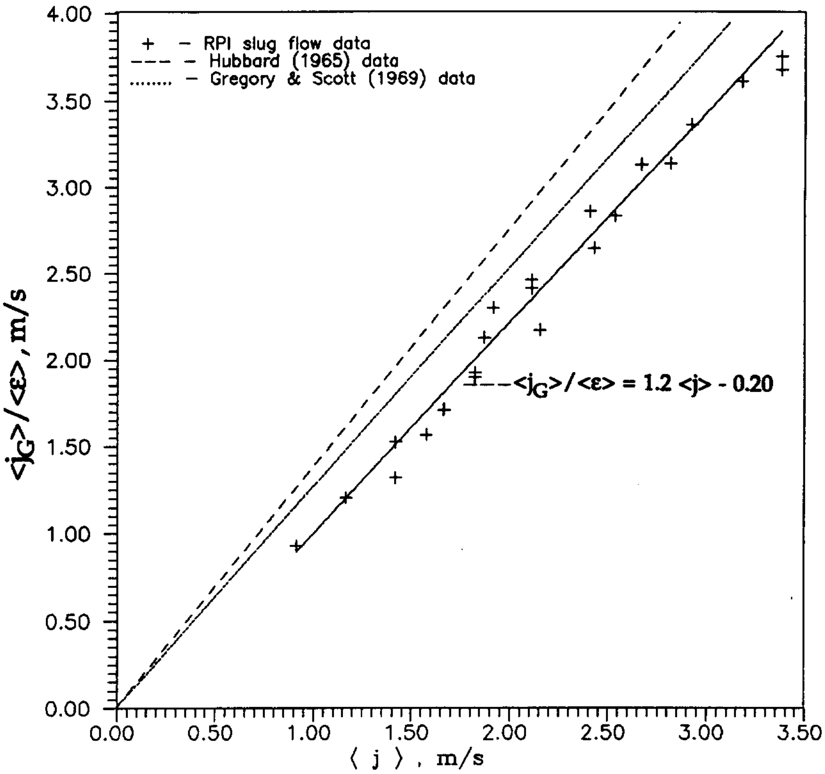

Figure 8. Slug flow data.

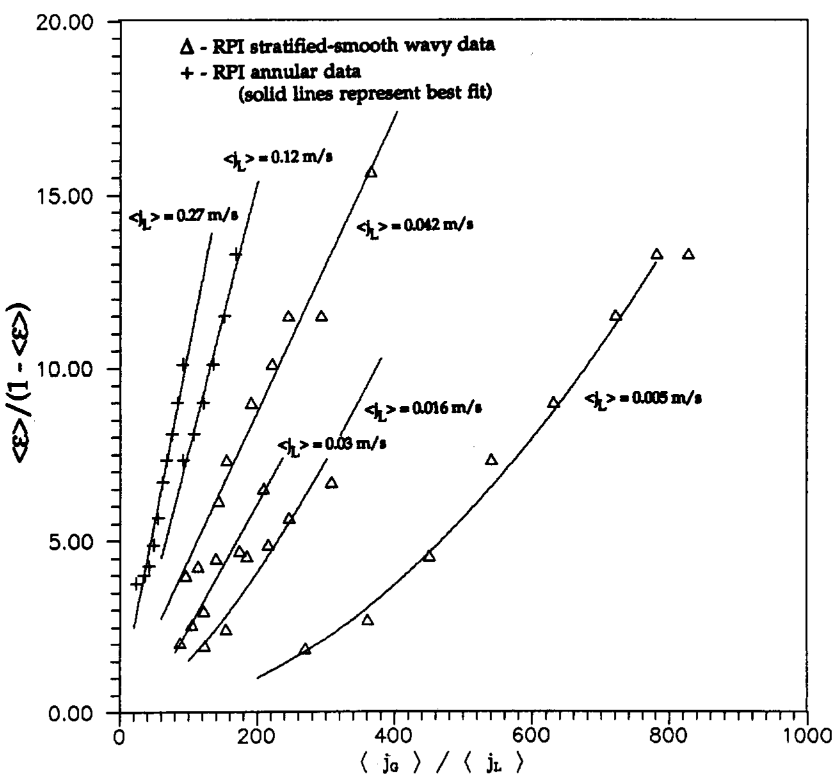

Figure 9. Wavy and annular flow data.

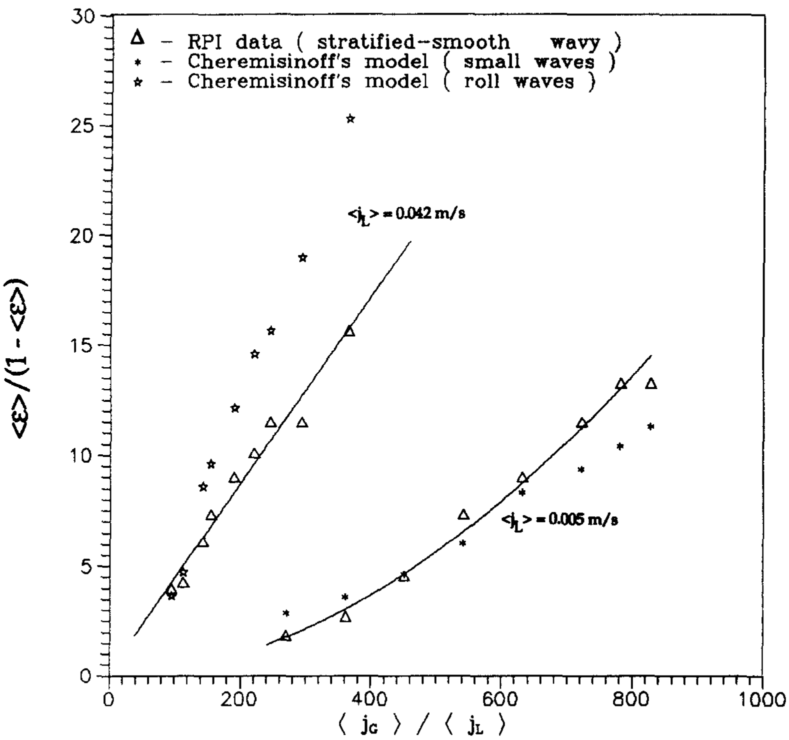

Figure 10. Comparison of RPI wavy flow data with the Cheremisinoff–Davis (1979) model.

the bubble velocity and the mixture velocity is linear, and yield $C_0 = 1.045$ and $V_{Gj} = 0.171$ m/s, for data taken in a 0.019 m dia horizontal conduit, with the superficial liquid velocity ranging from 0.3 to 1.5 m/s. It should be stressed that for horizontal flows the drift velocity, V_{Gj}, is not normally zero. The fact that many previous authors have assumed it to be zero just highlights their misunderstanding of what the drift velocity represents.

The drift-flux parameters for slug flow, given in figure 8, are distinctly different from those for plug flow. The higher value of $C_0(1.2)$ and the negative value for $V_{Gj}(-0.2$ m/s) can be explained by the displacement experienced by the gas bubble, its expansion due to a higher pressure drop and the liquid velocity distribution in the slug. In figure 7(b) we see that the nose of the bubble is displaced toward the center line of the pipe. The local liquid velocity profile is strongly distorted, because of drainage, and the liquid underneath the air bubble flows at a lower velocity than in the slug in front of it. The location of the peaks in the void and velocity profiles are thus closer, increasing the distribution coefficient, C_0. The liquid velocity profile in horizontal slug flow was measured by Kvernvold *et al.* (1984). One of their conclusions was that the velocity in the liquid film is mainly dependent on the liquid flow rate, while the velocity in the liquid slug increases strongly with increased gas flow rate.

The negative value for the drift velocity for slug flow implies that the local relative velocity, v_r, is negative. The data obtained by Bendiksen (1984) also show the same trend; a negative drift velocity at the highest liquid flow rates. It is worthwhile to mention that Hubbard (1965) and Gregory & Scott (1969) correlated slug flow as a linear function of v_b and $\langle j \rangle$, where v_b was defined as the bubble velocity. Their values for C_0 were 1.25 and 1.35, respectively, and the drift velocity was set to zero, based on (faulty) physical reasoning. The dotted lines in figure 8 represent their correlations.

Correlations for separated flows: wavy and annular patterns

In figure 9 the data for wavy and annular flow patterns were plotted using $\langle j_L \rangle$ as a parameter. The solid lines represent a best fit for each value of $\langle j_L \rangle$. As one would expect from drift-flux theory, when the liquid superficial velocity increases the experimental points were best fitted by straight lines. The drift velocity, calculated from the equation defining the coefficient K, [12], ranged

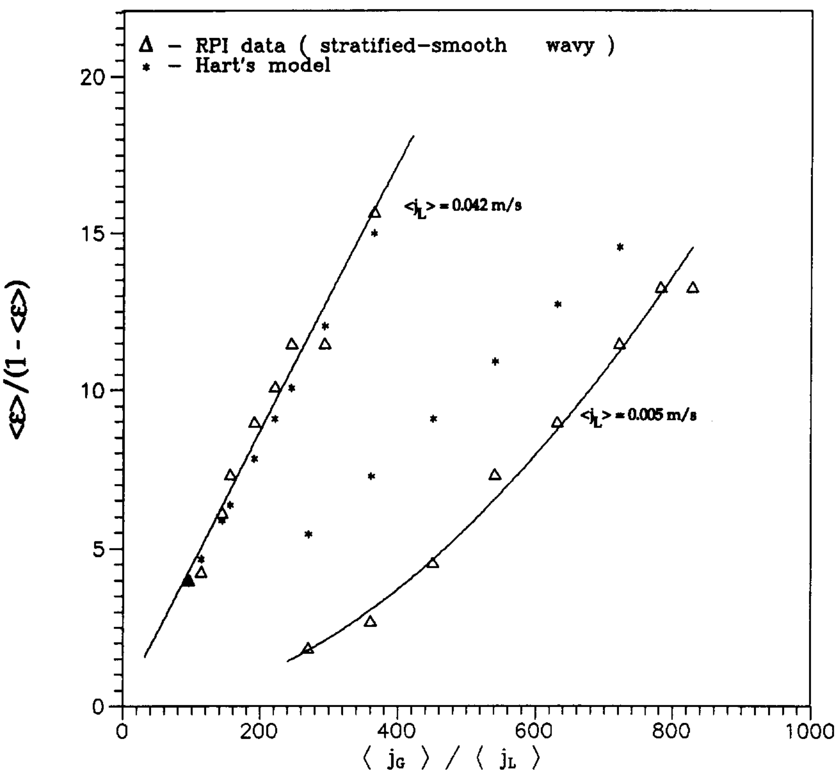

Figure 11. Comparison of wavy flow data with the Hart *et al.* (1989) model.

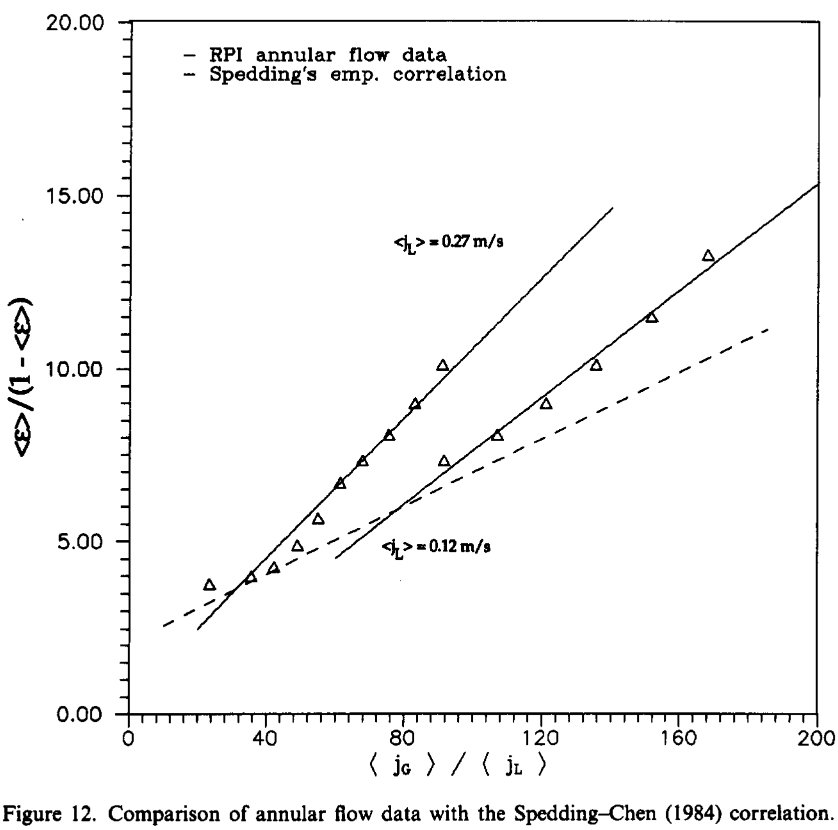

Figure 12. Comparison of annular flow data with the Spedding–Chen (1984) correlation.

Table 3

Flow regime	C_0	V_{Gj}(m/s)
Plug	$\cong 1.0$	0.16
Slug	1.2	-0.20
Wavy-stratified		0.2 for $\langle j_L \rangle = 0.005$ m/s
and annular	$\cong 1.0$	2.7 for $\langle j_L \rangle = 0.27$ m/s

from 0.2 to 2.7 m/s for $\langle j_L \rangle$ ranging from 0.005 to 0.27 m/s, respectively. For the lower liquid velocities, where most points represented stratified-smooth or two-dimensional wavy flow patterns, the best fit was obtained with power law curves.

Since data from other investigators were not available for wavy and annular patterns in the same range of flow variables, fluid properties and pipe configuration, results from models and correlations were used for comparison. In figure 10 we see a comparison between the present data and the Cheremisinoff–Davis (1979) model. The agreement is better for the lowest liquid velocity, when the model is evaluated for an interfacial friction factor related to two-dimensional waves. The authors have noted an average deviation from measured values $\leqslant 8\%$ for that condition.

As can be seen in figure 11, the model proposed by Hart *et al.* (1989), shows very good agreement with the present data at the higher liquid velocities. As mentioned previously, this model is particularly suitable for the wavy and annular flow regimes observed at those higher velocities. In figure 12, data for annular flows, fitted by straight lines, are compared to the Spedding–Chen (1984) correlation. It is apparent that the Spedding–Chen correlation shows the wrong trend.

CONCLUSION

It has been shown that horizontal two-phase flows can be well-correlated using a drift flux model. The standard variables, $\langle j_G \rangle / \langle \varepsilon \rangle$ and $\langle j \rangle$ can be used for plug and slug flows, while the other related variables, $\langle \varepsilon \rangle / (1 - \langle \varepsilon \rangle)$ and $\langle j_G \rangle / \langle j_L \rangle$, are more appropriate for stratified and annular flows. An objective criterion was proposed to differentiate between the plug and slug regimes, based on the phase which drives the flow. Unique sets of drift-flux parameters, C_0 and V_{Gj}, were obtained. The values obtained for the drift-flux parameters are given in table 3. It can be seen that these represent a self-consistent set of parameters and verify the validity of the drift-flux model for horizontal two-phase flows.

Acknowledgements—The financial support of this study by the National Science Foundation is gratefully acknowledged. In addition, the support of the Conselho Nacional de Desenvolvimento Científico e Tecnológico—CNPq, Brazil, which granted a scholarship to Professor F. França, is appreciated.

REFERENCES

Andreussi, P. & Persen, L. N. 1987 Stratified gas–liquid flow in downwardly inclined pipes. *Int. J. Multiphase Flow* **13,** 565–575.

Armand, A. A. 1946 The resistance during the movement of a two-phase system in horizontal pipes. *Izv. Vses. Teplotekh. Inst.* **1,** 16–23. *AERE Trans.* No. 828.

Beggs, H. D. 1972 An experimental study of two-phase flow in inclined pipes. Ph.D. Thesis, Univ. of Tulsa, OK.

Bendiksen, K. H. 1984 An experimental investigation of the motion of long bubbles in inclined tubes. *Int. J. Multiphase Flow* **10,** 467–483.

Butterworth, D. 1975 A comparison of some void-fraction relationships for co-current gas–liquid flow. *Int. J. Multiphase Flow* **1,** 845–850.

Chen, J. J. J. & Spedding, P. L. 1983 An analysis of holdup in horizontal two-phase gas–liquid flow. *Int. J. Multiphase Flow* **9,** 147–159.

Cheremisinoff, N. P. & Davis, E. J. 1979 Stratified turbulent–turbulent gas–liquid flow. *AIChE Jl* **25,** 48–56.

Cohen, L. S. & Hanratty, T. J. 1968 Effect of waves at a gas–liquid interface on a turbulent air flow. *J. Fluid Mech.* **31,** 467–476.

GOUVIER, G. W. & OMER, M. M. 1962 The horizontal pipeline flow of air–water mixtures. *Can. J. Chem. Engng* **June**, 93–104.

GREGORY, G. A. & SCOTT, D. S. 1969 Correlation of liquid slug velocity and frequency in horizontal co-current gas–liquid slug flow. *AIChE Jl* **15**, 933–935.

HART, J., HAMERSMA, P. J. & FORTUIN, J. M. H. 1989 Correlations predicting frictional pressure drop and liquid holdup during horizontal gas–liquid pipe flow with a small liquid holdup. *Int. J. Multiphase Flow* **15**, 947–964.

HUBBARD, M. G. 1965 An analysis of horizontal gas–liquid slug flow. Ph.D. thesis, Univ. of Houston, TX.

KVERNVOLD, O., VINDOY, V., SONTVEDT, T., SAASEN, A. & SELMER-OLSEN, S. 1984 Velocity distribution in horizontal slug flow. *Int. J. Multiphase Flow* **10**, 441–457.

LAHEY, R. T. JR & MOODY, F. J. 1977 The thermal-hydraulics of a boiling water nuclear reactor. ANS Monograph.

LOCKHART, R. W. & MARTINELLI, R. C. 1949 Proposed correlation of data for isothermal two-phase, two component flows in pipes. *Chem. Engng Prog.* **45**, 39–48.

NGUYEN, V. T. & SPEDDING, P. L. 1977 Holdup in two-phase, gas–liquid flow. *Nucl. Engng Sci.* **32**, 1003–1014.

SHOHAM, O. & TAITEL, Y. 1984 Stratified turbulent–turbulent gas–liquid flow in horizontal and inclined pipes. *AIChE Jl* **30**, 377–385.

SPEDDING, P. L. & CHEN, J. J. J. 1984 Hold-up in two-phase flow. *Int. J. Multiphase Flow* **10**, 307–339.

TAITEL, Y. & DUKLER, A. E. 1976 A model for predicting flow regime transitions in horizontal and near horizontal gas–liquid flow. *AIChE Jl* **22**, 47–55.

ZUBER, N. & FINDLAY, J. A. 1965 Average volumetric concentration in two-phase flow systems. *J. Heat Transfer* **Nov.**, 453–468.